Modeling and Control of Membranes for Gossamer Spacecraft Part 1: Theory

Marco Quadrelli[§] , Sam Sirlin
Autonomy & Control Section, Jet Propulsion Laboratory, California Institute of Technology, Pasadena, CA 91109

Abstract— **In this paper, Part 1 of 2, we derive the incremental equations of motion for a membrane to be used in simulations of gossamer spacecraft and, in particular, of precision inflatable structures. A boundary integral formulation is also presented, as a promising alternative to the finite element derivation. Some numerical results complete the paper. A discussion on control problems posed by large membrane structures in space will be the subject of Part 2.**

Keywords— **dynamics, control, membranes, inflatables, spacecraft.**

I. Introduction

The purpose of this paper is to shed some light on the dynamics and control problems one faces when modeling and analyzing gossamer-type spacecraft such as antennas built from inflatable structures, reflecting surfaces such as solar sails, and heat control surfaces such as solar shields. The term *gossamer* signifies *something light, delicate, insubstantial, or tenuous.* Examples are: a film of cobwebs floating in air; a large, ultra-lightweight system, packaged into a small launch volume. Typically, a gossamer spacecraft implies that its subsystems are highly-integrated with a thin structure performing multiple functions. It possesses extensive adaptive capabilities, eventually capable of reconfiguring or evolving in response to changing mission conditions. Because of these attributes, gossamer systems offer breakthrough reductions in mission cost.

Gossamer spacecraft at the present moment in time may be classified in those used for large apertures and in those used for solar sails and solar shields. Both types present their own problems when it comes to modeling, simulation, and control. Inflatable structures have been proposed as a low cost alternative for large apertures in space. One of the problems that inflatable large apertures present is the necessity of reaching a high surface accuracy for the inflated membrane reflector, in order for the antenna to perform satisfactorily at the required electromagnetic bandwidth. For a radio-interferometric mission such as ARISE (Advanced Radio Interferometry between Space and Earth), the expected surface accuracy error on the 25 meter inflatable dish is below 1 mm rms. Figure 1 shows the ARISE inflatable antenna, and points out some of the fields in which technological advancements are necessary for the mission to become a reality.

The effective surface accuracy of an inflatable antenna depends on many factors such as: systematic manufacturing errors, long-term ageing or creep of the polymeric membrane, quasi-static thermal distortions, and dynamic noise propagating from cooling equipment or attitude control devices. Even if in an ideal world most of these errors could be compensated by active means, there always remains a basic surface error. This surface error, expressed as some measure of difference between the real surface and the design paraboloid, is what the coefficients of the Zernike polynomial try to map. A pictorial representation of the first six Zernike polynomials for a circular optical element is depicted in Figure 2.

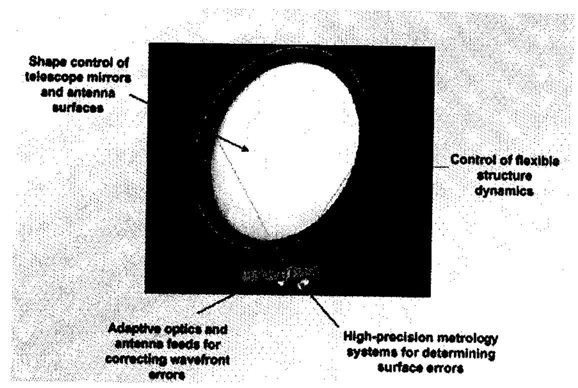

Figure 1. Interdisciplinary requirements for inflatable antennas.

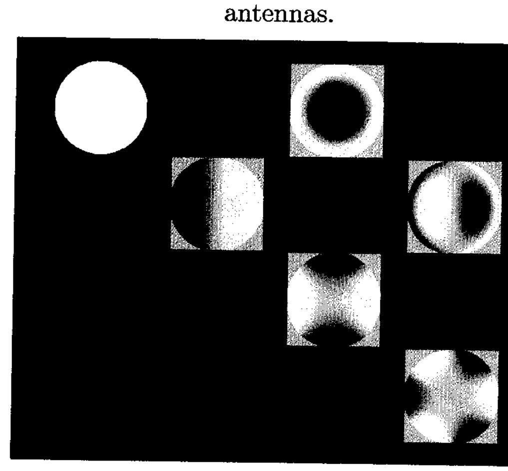

Figure 2. A pictorial representation of Zernike's polynomials.

Using a finite element method, we have derived the incremental equations of motion for a membrane to be used in

[§]corresponding author, marco@grover.jpl.nasa.gov

simulations of precision inflatable structures. A boundary integral formulaton has also been presented, as a promising alternative to the finite element derivation. We also summarize some of the modelling effort developed for the DRDF Contract *Shape Control of Inflatable Reflectors.*

Some membrane models will be discussed. The idea to develop these membrane models came from the need to have a simulation tool that can deal with the dynamics of membranes of inflatable structures, and with the following characteristics: orthotropic or homogeneous linear elastic material, large displacements and small strain. The prototype problem for such a membrane is an inflatable reflector which, after inflation, assumes the form of a paraboloid. Some studies have already been done on the inflation of an otherwise flat membrane into a paraboloid [Ref.[1]]. It turns out that a membrane that inflates is always under a certain amount of pre-tension, which ensures that the surface is reasonably free of wrinkles. Details of wrinkle modeling or of the inflation procedure are not within the scope of this study and require further investigation.

Of interest in this paper is the accuracy obtainable on the final shape of this surface after inflation, and also the method (or methods) to model and control this shape to a pre-specified accuracy. This is the essence of shape control.

This paper is divided into several sections. First, we deal with the basics of membranes subject to initial tension. Second, we develop a finite element model of the dynamics of a membrane that can be integrated in the MATLAB-based IMOS (Integrated Modeling of Optical Systems) software environment and that accurately models a membrane undergoing inflation. We divide the derivation in method of derivation, membrane kinematics, membrane dynamics, and finite element model. A later section of this paper deals with the validation of the element by comparing to previous results existing in the literature. Another section deals with alternative models which, because of time constraints, wait to be developed and implemented, but which have already been laid out theoretically. The conclusion and a list of references concludes this paper.

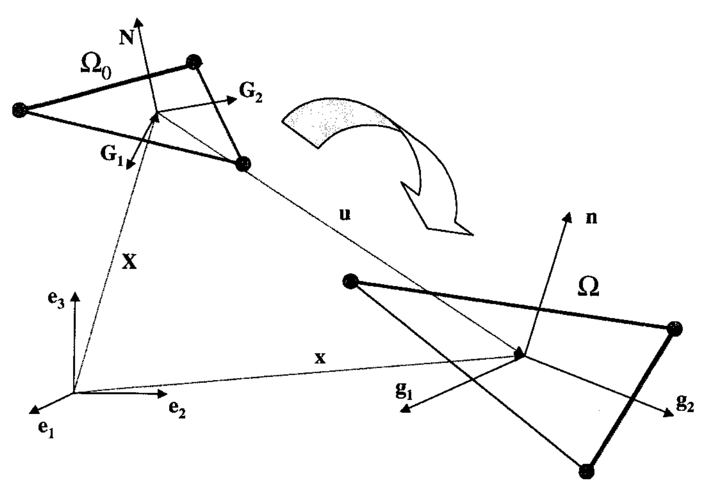

Figure 3. Kinematics of deformation of membrane element.

II. Modeling of an isotropic membrane subject to pressure, initial tension, and follower loads

We follow the development of [Ref.[3]] and the representation of Figure 3 for the nonlinear analysis of thin walled membranes with arbitrary geometry. We develop a displacement-based finite element interpolation scheme which includes the effects of initial tension, pressure load, and follower loads. Follower loads are included to represent actuator forces acting, to a first approximation, in the plane of the membrane. This is the case with embedded piezoelectrics.

A. Membrane kinematics

Our particular case is that in which we use cartesian rectangular coordinates (parameterized by the fixed basis vectors $\mathbf{e}_i$) to describe the geometry, and homogeneous, linear elastic constitutive equations. More details for the general case of material response can be found in [Ref. [3]]. An element of membrane of undeformed area and thickness $\{\Omega_0, h_0\}$ deforms into an element of area and thickness $\{\Omega, h\}$. We denote the undeformed configuration by $\mathcal{C}_u$ and the deformed configuration by $\mathcal{C}_d$. We are dealing with thin membranes, which means that the thickness is much smaller than the smallest radius of curvature of the membrane. We do not include bending effects. The inclusion of bending effects is unnecessary, since a membrane used for a space inflatable structure reacts only to in-plane loads. As a matter of fact, the inclusion of an initial pretension load is required for the membrane to be able to support a minimum of bending stiffness (think of the membrane of a drum), or to be able to support a vertical load. A point (ξ, η) of the membrane surface initially located at $\mathbf{X}$=$\mathrm{X}_i\mathbf{e}_i$ gets displaced into a point located at

$$\mathbf{x} = \mathbf{X} + \mathbf{u} = \mathbf{x_i e_i} \tag{1}$$

where $\mathbf{u}$ is the displacement vector. The membrane may have initial curvature, therefore initial base vectors $\mathbf{G_1} = \frac{\partial \mathbf{X}}{\partial \xi}$ and $\mathbf{G_2} = \frac{\partial \mathbf{X}}{\partial \eta}$ can be derived. For an initially flat membrane, they are $\mathbf{G_1} = \begin{pmatrix} 1 & 0 & 0 \end{pmatrix}$ and $\mathbf{G_2} = \begin{pmatrix} 0 & 1 & 0 \end{pmatrix}$ since $\xi = x$ and $\eta = y$. In the deformed configuration, we also have:

$$\mathbf{g_1} = \mathbf{X}_{,1} + \mathbf{u}_{,1} = \begin{pmatrix} 1 + \frac{\partial u}{\partial x} & \frac{\partial v}{\partial x} & \frac{\partial w}{\partial x} \end{pmatrix} \tag{2}$$

$$\mathbf{g_2} = \mathbf{X}_{,2} + \mathbf{u}_{,2} = \begin{pmatrix} \frac{\partial u}{\partial y} & 1 + \frac{\partial v}{\partial y} & \frac{\partial w}{\partial y} \end{pmatrix} \tag{3}$$

where (u, v, w) denote the components of the displacement vector $\mathbf{u}$ in cartesian rectangular coordinates. The metric coefficients of the undeformed and deformed membrane surface can then be written as $(\alpha, \beta = 1, 2)$:

$$G_{\alpha\beta} = \mathbf{X}_{,\alpha} \cdot \mathbf{X}_{,\beta} \tag{4}$$

$$g_{\alpha\beta} = \mathbf{x}_{,\alpha} \cdot \mathbf{x}_{,\beta} \tag{5}$$

and allow the definition of the membrane strain tensor

$$E_{\alpha\beta} = \frac{1}{2}\left(g_{\alpha\beta} - G_{\alpha\beta}\right) \tag{6}$$

The strain tensor components can be assembled in vector form as follows:

$$\mathbf{E} = \begin{pmatrix} E_{11} & E_{22} & E_{12} \end{pmatrix} \tag{7}$$

Since we adopt a finite element interpolation scheme, we can write

$$\mathbf{u} = \mathbf{S}\mathbf{q} \tag{8}$$

where $\mathbf{S}$ is a matrix of interpolation coefficients, and $\mathbf{q}$ the vector of nodal displacements.

B. Membrane kinetics

To describe the kinetics of the membrane, we use the Principle of Virtual Work, which states that for any admissible displacement field $\mathbf{u}$, the membrane deforms to external loads so as the following variational functional is made stationary:

$$\begin{aligned} G_{dyn}(\mathbf{u}, \boldsymbol{\delta}\mathbf{u}) \;=\; & \int_{\Omega_0} h_0 \rho_0 \ddot{\mathbf{u}} \cdot \boldsymbol{\delta}\mathbf{u} d\boldsymbol{\Omega}_0 + \\ & \int_{\Omega_0} h_0 \mathbf{S} \cdot \boldsymbol{\delta}\mathbf{E} d\boldsymbol{\Omega}_0 - \\ & \int_{\Omega_0} h_0 p\mathbf{n} \cdot \boldsymbol{\delta}\mathbf{u} d\boldsymbol{\Omega}_0 - \\ & \int_{\Omega_0} h_0 \mathbf{f_e} \cdot \boldsymbol{\delta}\mathbf{u} d\boldsymbol{\Omega}_0 \end{aligned} \tag{9}$$

where: $\delta\mathbf{u}$ is a displacement test vector function, ρ_0 is the material density in $\mathcal{C}_d$, $\ddot{\mathbf{u}}$ the translational acceleration of a point, $\mathbf{S}$ the second Piola-Kirchhoff stress tensor, $\mathbf{E}$ the membrane strain tensor, p is the scalar pressure, $\mathbf{n}$ is the vector normal to the surface in $\mathcal{C}_d$, and $\mathbf{f_e}$ is the vector of external conservative or non-conservative (i.e., follower) forces acting on the membrane. Any forces due to control action are represented by $\mathbf{f_e}$.

Let us summarize the development we are after in the case of linear material response and small deformations.

Initial tension effects are a very crucial issue and may significantly change the natural frequencies of the antenna dish compared to the case in which initial tension is absent. From a structural point of view, the work done by the internal forces is composed of three additive terms:

- internal work due to the material properties, which comes only from the linear part of the constitutive relationship between stresses and strain, and which is constant for a linearly elastic (even orthotropic) material;
- internal work due to initial displacements;
- internal work due to the initial force and moment components.

Assuming that the initial configuration of the membrane is statically equilibrated, the contribution of the initial displacements is zero.

From a finite element point of view, the material and initial load work become the (linear) material stiffness matrix and the geometrical stiffness matrix. In general, the geometrical stiffness matrix, which depends on the load, is also configuration dependent, in the sense that it also depends on the rotational degrees of freedom in a very non-linear fashion. In the case we restrict ourselves to linear structural dynamics, we must impose that the nodal rotations θ are small, i.e., such that $sin\theta \approx \theta$.

In the case of the membrane reflector, the initial load acts in the plane of the membrane with three components, i.e. the force resultant in the x direction N_x, the force resultant in the y direction N_y, and the shear force resultant $N_x y$. Although the initial shape is curved, the deformation pattern should be such that the maximum angular deformation is extremely small. The pre-load applied by the turnbuckles ensures this. Since there are no localized forces perpendicular to the plane of the membrane (only distributed pressures of very low intensity compared to the lateral pre-load), and the thickness is very small, the response is localized to the membrane plane as a state of plane stress. A membrane model is more adequate than a shell model, since we expect the bending response to be a lot more negligible than the in-plane axial response, and because large rotations due to bending action do not take place.

The problem is now reduced to that of designing a linear elastic membrane element, with small rotational deformation, and subject to the effect of the initial in plane load, pressure load, and follower forces.

The equilibrium equations of an element of the membrane initially located on the x-y plane are

$$\frac{\partial N_x}{\partial x} + \frac{\partial N_{xy}}{\partial y} + p_x = 0 \tag{10}$$

in the x direction,

$$\frac{\partial N_{xy}}{\partial x} + \frac{\partial N_y}{\partial y} + p_y = 0 \tag{11}$$

in the y direction, and

$$\frac{\partial}{\partial x}(N_x \frac{\partial z}{\partial x} + N_{xy} \frac{\partial z}{\partial y}) + \frac{\partial}{\partial y}(N_{xy} \frac{\partial z}{\partial x} + N_y \frac{\partial z}{\partial y}) + p_z = 0 \tag{12}$$

in the z direction, where

$$N_x = \int_t \sigma_{xx} dz \tag{13}$$

$$N_y = \int_t \sigma_{yy} dz \tag{14}$$

$$N_{xy} = N_{yx} = \int_t \sigma_{xy} dz \tag{15}$$

and t is the membrane thickness. Neglecting terms of order higher than the second, the strain-displacement relationships are:

$$\epsilon_{xx} = E_{11} = \frac{\partial u}{\partial x} + \frac{1}{2}\left[(\frac{\partial u}{\partial x})^2 + (\frac{\partial v}{\partial x})^2 + (\frac{\partial w}{\partial x})^2\right] \tag{16}$$

$$\epsilon_{yy} = E_{22} = \frac{\partial v}{\partial y} + \frac{1}{2}\left[(\frac{\partial u}{\partial y})^2 + (\frac{\partial v}{\partial y})^2 + (\frac{\partial w}{\partial y})^2\right] \tag{17}$$

$$\epsilon_{xy} = 2E_{12} = \frac{\partial v}{\partial x} + \frac{\partial u}{\partial y} + \frac{\partial u}{\partial x}\frac{\partial u}{\partial y} + \frac{\partial v}{\partial x}\frac{\partial v}{\partial y} + \frac{\partial w}{\partial x}\frac{\partial w}{\partial y} \quad (18)$$

The presence of the squared terms is necessary to incorporate the effect of the initial tension. In fact, neglecting some small terms, the potential energy contribution associated with the initial stress effect is given by

$$V = \frac{h_0}{2}\int_V [N_x(\frac{\partial w}{\partial x})^2 + N_y(\frac{\partial w}{\partial y})^2 + 2N_{xy}\frac{\partial w}{\partial x}\frac{\partial w}{\partial y}]dxdy \quad (19)$$

The resultant membrane element stiffness matrix is given by the term caused by the initial stresses, which results in contributions to the nodal rotations θ_x and θ_y components, in addition to the linear elastic term which because of the plane stress assumption acts on the nodal u and v components.

Once the membrane element has been modified this way, a procedure is needed to compute the initial stresses. This procedure can only be iterative in nature, but a first order approximate solution would include a constant load at the membrane rim location. This constant load is caused by the pretension at the constant force springs, may be assumed equal to a constant value at the beginning of the simulation, and consists of a radial and a circumferential component. Given the load on the rim, an equilibrium solution can be computed for the whole membrane at the initial step, and the resulting static deformation of the membrane surface will not change in time. A more accurate analysis of the deformation of the membrane requires the updating of the deformation of the membrane during simulation. This is an iterative process, and should also include the initial stress terms in the struts and torus which provide structural support for the membrane. Therefore, an initial stress matrix needs to be derived also for the beam elements which model the struts. Again, this initial stress stiffness matrix acts on the rotational degrees of freedom associated with each beam element.

Note that the effect of material orthotropy enters the elastic stiffness matrix. This matrix needs to be rederived for orthotropy, but it can be done in a straightforward manner since the difference with respect to the case of isotropy lies only in a different constitutive tensor linking stress to strain components.

C. Residual and Tangent Stiffness derivation

Upon linearizing 9 by taking the directional derivative in the direction of an increment $\mathbf{\Delta u}$, we obtain the following result:

$$\begin{aligned}\Delta G_{dyn}(\mathbf{u},\boldsymbol{\delta}\mathbf{u})\cdot\mathbf{\Delta u} \quad = \quad & \int_{\Omega_0} h_0\rho_0 \mathbf{\Delta \ddot{u}}\cdot\boldsymbol{\delta}\mathbf{u}d\boldsymbol{\Omega}_0 + \quad (20)\\ & \int_{\Omega_0} h_0 \mathbf{\Delta S}\cdot\boldsymbol{\delta}\mathbf{E}d\boldsymbol{\Omega}_0 + \\ & \int_{\Omega_0} h_0 \mathbf{S}\cdot\boldsymbol{\delta}\mathbf{\Delta E}d\boldsymbol{\Omega}_0 - \\ & \int_{\Omega_0} h_0 p\mathbf{\Delta n}\cdot\boldsymbol{\delta}\mathbf{u}d\boldsymbol{\Omega}_0 - \\ & \int_{\Omega_0} h_0 \mathbf{\Delta f_e}\cdot\boldsymbol{\delta}\mathbf{u}d\boldsymbol{\Omega}_0\end{aligned}$$

Upon substituting equation 8 into 9, we derive the tangent matrices as follows. The first term of this expression leads to the inertia matrix. The second term leads to the material stiffness matrix. The third term leads to the geometric stiffness matrix. The fourth term leads to the pressure stiffness matrix. The last term leads to the follower load matrix. Equation 9 also represents the work performed by the residual generalized forces acting on the structure any time the displacement variation $\delta\mathbf{u}$ from any intermediate equilibrium configuration is different from zero. Therefore equation 9 defines the residual load vector.

The total stiffness matrix is given by

$$\mathbf{K_T} = \mathbf{K_e} + \mathbf{K}_\sigma + \mathbf{K_p} + \mathbf{K_f} \quad (21)$$

and is obviously unsymmetric on account of the pressure and follower loads.

C.1 Inertia matrix

The inertia matrix is simply:

$$\mathbf{M} = \int_{\Omega_0} \mathbf{h}_0\boldsymbol{\rho}_0\mathbf{S^T}\cdot\mathbf{S}d\boldsymbol{\Omega}_0 \quad (22)$$

C.2 Material stiffness matrix

To compute the material stiffness matrix, we need the constitutive equation. For a homogeneous, isotropic, and linear elastic material, the constitutive equation may be written as

$$\mathbf{S} = \mathbf{C}\cdot\mathbf{E} \quad (23)$$

where $\mathbf{C}$ is a matrix derived from the elasticity tensor, and which contains terms depending only on the Young's modulus E and Poisson's ratio ν. The strain-displacement relationship is also needed. The exact representation is given in equations 16, 17, and 18. The linear strain vector does not include any contribution from the displacement w, and may be written as:

$$\mathbf{E_{lin}} = \begin{pmatrix} N_{u,x} & N_{v,y} & \frac{1}{2}(N_{u,y}+N_{v,x}) \end{pmatrix}\mathbf{q} \quad (24)$$

where $N_{u,x}$ and $N_{v,y}$ represent the derivatives of the shape functions associated with the u and v displacements. In incremental form:

$$\mathbf{\Delta E_{lin}} = \mathbf{BS\Delta q} \quad (25)$$

where $\mathbf{B}$ is an operator matrix. Consequently, the linear elastic material stiffness matrix becomes:

$$\mathbf{K_e} = \int_{\Omega_0} \mathbf{h}_0\mathbf{L^T C L}d\boldsymbol{\Omega}_0 \quad (26)$$

where $\mathbf{L} = \begin{pmatrix} N_{u,x} & N_{v,y} & \frac{1}{2}(N_{u,y}+N_{v,x}) \end{pmatrix}$. Since naturally a membrane has no stiffness in the w direction, there is no contribution from the w displacement.

C.3 Geometric stiffness matrix

The nonlinear terms of the strain tensor may be written as follows:

$$\mathbf{E}_{\mathbf{nonlin}} = \frac{1}{2}\begin{pmatrix} \mathbf{q}^{\mathbf{T}}\left(\mathbf{N}_{\mathbf{u,x}}^{\mathbf{T}}\mathbf{N}_{\mathbf{u,x}} + \mathbf{N}_{\mathbf{v,x}}^{\mathbf{T}}\mathbf{N}_{\mathbf{v,x}} + \mathbf{N}_{\mathbf{w,x}}^{\mathbf{T}}\mathbf{N}_{\mathbf{w,x}}\right)\mathbf{q} \\ \mathbf{q}^{\mathbf{T}}\left(\mathbf{N}_{\mathbf{u,y}}^{\mathbf{T}}\mathbf{N}_{\mathbf{u,y}} + \mathbf{N}_{\mathbf{v,y}}^{\mathbf{T}}\mathbf{N}_{\mathbf{v,y}} + \mathbf{N}_{\mathbf{w,y}}^{\mathbf{T}}\mathbf{N}_{\mathbf{w,y}}\right)\mathbf{q} \\ \mathbf{q}^{\mathbf{T}}\left(\mathbf{N}_{\mathbf{u,x}}^{\mathbf{T}}\mathbf{N}_{\mathbf{u,y}} + \mathbf{N}_{\mathbf{v,x}}^{\mathbf{T}}\mathbf{N}_{\mathbf{v,y}} + \mathbf{N}_{\mathbf{w,x}}^{\mathbf{T}}\mathbf{N}_{\mathbf{w,y}}\right)\mathbf{q} \end{pmatrix}^{T} \quad (27)$$

and

$$\Delta\mathbf{E}_{\mathbf{nonlin}} = \frac{\partial\mathbf{E}_{\mathbf{nonlin}}}{\partial\mathbf{q}}\boldsymbol{\Delta}\mathbf{q} \quad (28)$$

or

$$\begin{aligned} \Delta\mathbf{E}_{\mathbf{nonlin_{11}}} &= \mathbf{q}^{\mathbf{T}}\left(\mathbf{N}_{\mathbf{u,x}}^{\mathbf{T}}\mathbf{N}_{\mathbf{u,x}} + \mathbf{N}_{\mathbf{v,x}}^{\mathbf{T}}\mathbf{N}_{\mathbf{v,x}} + \mathbf{N}_{\mathbf{w,x}}^{\mathbf{T}}\mathbf{N}_{\mathbf{w,x}}\right) \\ &\quad \cdot\boldsymbol{\Delta}\mathbf{q} \quad (29) \\ &= \mathbf{q}^{\mathbf{T}}\mathbf{G}_{11}\boldsymbol{\Delta}\mathbf{q} \\ \Delta\mathbf{E}_{\mathbf{nonlin_{22}}} &= \mathbf{q}^{\mathbf{T}}\mathbf{G}_{22}\boldsymbol{\Delta}\mathbf{q} \\ \Delta\mathbf{E}_{\mathbf{nonlin_{12}}} &= \mathbf{q}^{\mathbf{T}}\mathbf{G}_{12}\boldsymbol{\Delta}\mathbf{q} \end{aligned}$$

$$\begin{aligned} \delta\Delta\mathbf{E}_{\mathbf{nonlin_{11}}} &= \delta\mathbf{q}^{\mathbf{T}}\mathbf{G}_{11}\boldsymbol{\Delta}\mathbf{q} \\ \delta\Delta\mathbf{E}_{\mathbf{nonlin_{22}}} &= \delta\mathbf{q}^{\mathbf{T}}\mathbf{G}_{22}\boldsymbol{\Delta}\mathbf{q} \\ \delta\Delta\mathbf{E}_{\mathbf{nonlin_{12}}} &= \delta\mathbf{q}^{\mathbf{T}}\mathbf{G}_{12}\boldsymbol{\Delta}\mathbf{q} \end{aligned} \quad (30)$$

Therefore, we can write that the internal work contribution is as follows:

$$\begin{aligned} &\boldsymbol{\Delta}\int_{\boldsymbol{\Omega}_0}\mathbf{h}_o\mathbf{S}\cdot\boldsymbol{\delta}\mathbf{E}\mathbf{d}\boldsymbol{\Omega}_0 \\ =& \int_{\Omega_0} h_o\Delta\mathbf{S}\cdot\boldsymbol{\delta}\mathbf{E}\mathbf{d}\boldsymbol{\Omega}_0 + \int_{\boldsymbol{\Omega}_0}\mathbf{h}_o\mathbf{S}\cdot\boldsymbol{\delta\Delta}\mathbf{E}\mathbf{d}\boldsymbol{\Omega}_0 = \\ &\int_{\Omega_0} h_o\left(\Delta\mathbf{E}_{\mathbf{lin}}^{\mathbf{T}}\mathbf{C}\boldsymbol{\delta}\mathbf{E}_{\mathbf{lin}}\right)d\Omega_0 + \\ &\int_{\Omega_0} h_o\left(\Delta\mathbf{E}_{\mathbf{lin}}^{\mathbf{T}}\mathbf{C}\boldsymbol{\delta}\mathbf{E}_{\mathbf{nonlin}}\right)d\Omega_0 + \\ &\int_{\Omega_0} h_o\left(\Delta\mathbf{E}_{\mathbf{nonlin}}^{\mathbf{T}}\mathbf{C}\boldsymbol{\delta}\mathbf{E}_{\mathbf{lin}}\right)d\Omega_0 + \\ &\int_{\Omega_0} h_o\left(\Delta\mathbf{E}_{\mathbf{nonlin}}^{\mathbf{T}}\mathbf{C}\boldsymbol{\delta}\mathbf{E}_{\mathbf{nonlin}}\right)d\Omega_0 + \\ &\int_{\Omega_0} h_o\left(\mathbf{S}^{\mathbf{T}}\boldsymbol{\delta\Delta}\mathbf{E}_{\mathbf{lin}}\right)d\Omega_0 + \\ &\int_{\Omega_0} h_o\left(\mathbf{S}^{\mathbf{T}}\boldsymbol{\delta\Delta}\mathbf{E}_{\mathbf{nonlin}}\right)d\Omega_0 \end{aligned} \quad (31)$$

The first term is the linear elastic material stiffness matrix. The geometric stiffness matrix is therefore derived as:

$$\begin{aligned} \mathbf{K}_\sigma &= \int_{\Omega_0} h_o\left(\mathbf{S}^{\mathbf{T}}\boldsymbol{\delta\Delta}\mathbf{E}_{\mathbf{lin}}\right)d\Omega_0 \quad (32) \\ &\quad + \int_{\Omega_0} h_o\left(\mathbf{S}^{\mathbf{T}}\boldsymbol{\delta\Delta}\mathbf{E}_{\mathbf{nonlin}}\right)d\Omega_0 \\ &= \int_{\Omega_0} h_o\left(\mathbf{S}^{\mathbf{T}}\boldsymbol{\delta\Delta}\mathbf{E}_{\mathbf{nonlin}}\right)d\Omega_0 \end{aligned}$$

Using 30, we obtain:

$$\mathbf{K}_\sigma = \int_{\boldsymbol{\Omega}_0}\mathbf{h}_o\left(\mathbf{S}_{11}\mathbf{G}_{11} + \mathbf{S}_{22}\mathbf{G}_{22} + 2\mathbf{S}_{12}\mathbf{G}_{12}\right)\mathbf{d}\boldsymbol{\Omega}_0 \quad (33)$$

The remaining terms in 31 pertain to a true nonlinear analysis, and are higher order displacement-dependent matrices which we neglect since we adopt an incremental solution method.

C.4 Pressure load stiffness matrix

The pressure load stiffness matrix needs a particular derivation. First, the unit vector normal to the deformed surface can be written as:

$$\mathbf{n} = \frac{\mathbf{g}_1\times\mathbf{g}_2}{|\mathbf{g}_1\times\mathbf{g}_2|} \quad (34)$$

and the deformed element area is

$$d\Omega = \frac{|\mathbf{g}_1\times\mathbf{g}_2|}{|\mathbf{G}_1\times\mathbf{G}_2|}d\Omega_0 \quad (35)$$

so that the incremental work due to pressure is

$$\Delta\delta\Pi_p\cdot\delta\mathbf{u} = -\int_{\boldsymbol{\Omega}_0}\mathbf{h}_o\frac{\left(|\boldsymbol{\Delta}\mathbf{g}_1\times\mathbf{g}_2| + |\mathbf{g}_1\times\boldsymbol{\Delta}\mathbf{g}_2|\right)}{|\mathbf{G}_1\times\mathbf{G}_2|}\cdot\boldsymbol{\delta}\mathbf{u}\mathbf{d}\boldsymbol{\Omega}_0 \quad (36)$$

Here, $\Delta\mathbf{g}_\alpha = \mathbf{H}_\alpha\boldsymbol{\Delta}\mathbf{q}$ and

$$\Delta\mathbf{g}_1\times\mathbf{g}_2 = \left[-\left(\mathbf{H}_2\mathbf{q}\right)^\times\mathbf{H}_1\right]\boldsymbol{\Delta}\mathbf{q} = \mathbf{F}_1\boldsymbol{\Delta}\mathbf{q} \quad (37)$$

$$\mathbf{g}_1\times\boldsymbol{\Delta}\mathbf{g}_2 = \left[\left(\mathbf{H}_1\mathbf{q}\right)^\times\mathbf{H}_2\right]\boldsymbol{\Delta}\mathbf{q} = \mathbf{F}_2\boldsymbol{\Delta}\mathbf{q} \quad (38)$$

where $(\cdot)^\times$ denotes the skew-symmetric matrix associated with the vector $(\cdot)$. Consequently, the pressure load matrix becomes:

$$\mathbf{K}_\mathbf{p} = -\int_{\boldsymbol{\Omega}_0}\mathbf{h}_o\mathbf{p}\left(\mathbf{F}_1+\mathbf{F}_2\right)^{\mathbf{T}}\mathbf{S}\mathbf{d}\boldsymbol{\Omega}_0 \quad (39)$$

C.5 Follower load stiffness matrix

The follower load stiffness matrix also requires a special derivation. In incremental form, we have that the work is

$$\Delta\delta\Pi_f\cdot\delta\mathbf{u} = -\int_{\boldsymbol{\Omega}_0}\mathbf{h}_o\boldsymbol{\Delta}\mathbf{f}_\mathbf{e}\cdot\boldsymbol{\delta}\mathbf{u}\frac{|\mathbf{g}_1\times\mathbf{g}_2|}{|\mathbf{G}_1\times\mathbf{G}_2|}\mathbf{d}\boldsymbol{\Omega}_0 \quad (40)$$

But for conservative forces (i.e., their direction is always along the $\mathbf{e}_i$ basis)

$$\mathbf{f}_\mathbf{e} = \mathbf{f}_{\mathbf{e}_1}\frac{\mathbf{G}_1}{|\mathbf{G}_1|} + \mathbf{f}_{\mathbf{e}_2}\frac{\mathbf{G}_2}{|\mathbf{G}_2|} \quad (41)$$

whereas for non-conservative or follower forces (i.e., their direction follows the deformation)

$$\mathbf{f}_\mathbf{e} = \mathbf{f}_{\mathbf{e}_1}\frac{\mathbf{g}_1}{|\mathbf{g}_1|} + \mathbf{f}_{\mathbf{e}_2}\frac{\mathbf{g}_2}{|\mathbf{g}_2|} \quad (42)$$

Also,

$$\Delta \mathbf{f_e} = \mathbf{f_{e_1}} \mathbf{\Delta} \left(\frac{\mathbf{g_1}}{|\mathbf{g_1}|} \right) + \mathbf{f_{e_2}} \mathbf{\Delta} \left(\frac{\mathbf{g_2}}{|\mathbf{g_2}|} \right) = \mathbf{\Xi} \ \mathbf{\Delta q} \tag{43}$$

and the follower load stiffness is

$$\mathbf{K_f} = - \int_{\Omega_0} \mathbf{h_o} \mathbf{\Xi^T S} \frac{|\mathbf{g_1} \times \mathbf{g_2}|}{|\mathbf{G_1} \times \mathbf{G_2}|} \mathbf{d\Omega_0} \tag{44}$$

From 43, we have that

$$\Delta \left(\frac{\mathbf{g_1}}{|\mathbf{g_1}|} \right) = \left[\frac{\mathbf{H_1}}{|\mathbf{g_1}|} - \frac{(\mathbf{g_1} \cdot \mathbf{H_1})\, \mathbf{g_1}}{(|\mathbf{g_1}|)^3} \right] \Delta \mathbf{q} = \mathbf{T_1 \Delta q} \tag{45}$$

$$\Delta \left(\frac{\mathbf{g_2}}{|\mathbf{g_2}|} \right) = \mathbf{T_2 \Delta q} \tag{46}$$

and consequently

$$\mathbf{\Xi} = \mathbf{f_{e_1} T_1} + \mathbf{f_{e_2} T_2} \tag{47}$$

For conservative forces, there is no tangent stiffness matrix, and the residual vector takes the general form

$$\mathbf{F_i} = \int_{\Omega_0} \mathbf{h_o S^T f_e} \frac{|\mathbf{g_1} \times \mathbf{g_2}|}{|\mathbf{G_1} \times \mathbf{G_2}|} \mathbf{d\Omega_0} \tag{48}$$

III. Modeling of wrinkling in the membrane

This section is purely descriptive, and for illustrative purposes only. A photograph of a Fluorinated Polymide film with embedded rip-stops, used in inflatable spacecraft work, is shown in Figure 4. One may notice the extensive wrinkling present in the surface. These wrinkles partially disappear when the film is subjected to gas pressure from the inflation equipment. More generally, some wrinkles remain after inflation that have to be eliminated actively. When the film is packaged and folded, occasional creases may form, which sometimes are conducive to local cracking and peeling. This is of course a very negative condition, as cracks and puncturing in the film are also sources of localized electrostatic charging, and arcing may also occur with destructive effects for the whole structure.

There are two different schools of thought that have dealt with the modeling of wrinkling membranes. One school of thought [Roddeman, Schrefler, et al.] solve the problem by traditional finite elements. However, the second derivative of the strain energy becomes ill-conditioned when a part of the structure becomes slack once a wrinkle has formed, because the elastic moduli vary discontinuously across the boundaries of various sub-domains in strain space that comprise the domain of the strain energy function. Therefore these finite element based methods typically involve iterative algorithms that eliminate compressive stress in each stage of an incremental loading procedure. Another school of thought [Pipkin, Steigmann, et al.] is based on the concept of a relaxed strain energy. This is a reformulation of the problem so that the strain energy takes different forms in different regions of strain space, associated with the state of strain corresponding to a tense, wrinkled, or completely slack condition. The construction of the composite strain energy function is determined a priori from minimum energy considerations. When the relaxed strain energy is used, compressive stresses are excluded automatically. A future paper will deal with wrinkling modeling and control of wrinkling processes in ultra-lightweight space vehicles.

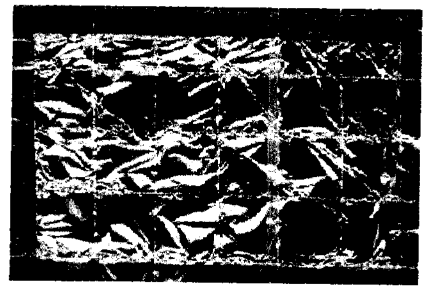

Figure 4. What a Fluorinated Polyimide film with embedded rip-stops looks like.

IV. Boundary Integral Formulation

In this section, we describe a theoretical development which can be applied to the development of efficient shallow shell elements. Although in this paper we focus on membrane models, this is section applies to shells, i.e. material surfaces where bending deformation are not entirely negligible. In this derivation, we adopt a boundary integral approach with the objective in mind of developing a more efficient finite element interpolation scheme with less number of nodes (boundary integral formulations have the advantage of reduced dimensionality since they retain boundary nodes only, and assume an exact solution in the interior of the domain). Furthermore, we adopt a mixed variational formulation, in which not only displacements, but also stresses are interpolated. A mixed method has the advantage that it is equivalent to a reduced integration of the bending terms. Consequently, the ubiquitous shear locking problem of shells is entirely avoided. This result in a very efficient interpolation scheme for dynamics analysis of membranes in which bending action is not entirely negligible.

We assume a shallow shell theory, i.e. the deviation of the real surface from a flat surface is small compared to the principal curvatures. See Figure 5. We assume homogeneous, isotropic, linear elastic material, negligible shear deformation and rotary inertia, constant thickness.

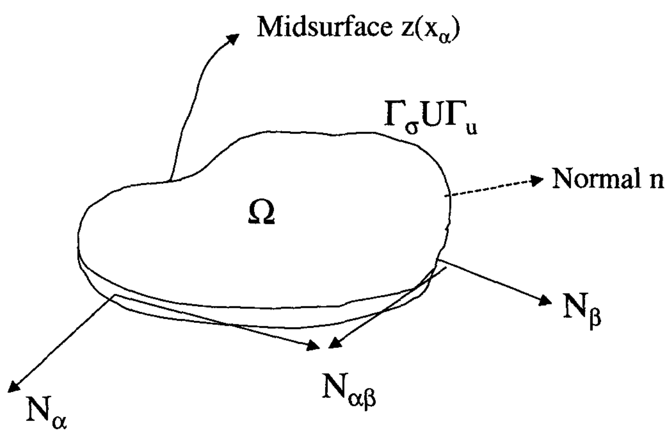

Figure 5. Surface stresses in shallow shell

Denoting quantities on the shell surface identified by its midsurface $z = z(x_\alpha)$ by the subscripts (α, $\beta = 1, 2$), and by $R_{\alpha\beta}$ the initial curvatures, we may write the strain-displacement, or compatibility equations as:

$$\varepsilon_{\alpha\beta} = \frac{1}{2}\left(u_{,\alpha} + u_{,\beta} + w_{,\alpha}w_{,\beta} + \frac{2w}{R_{\alpha\beta}}\right) \tag{49}$$

where $\varepsilon_{\alpha\beta}$ are the components of the strain tensor and $R_{\alpha\beta} = -\frac{1}{z_{,\alpha\beta}}$. The constitutive equations can be written as:

$$N_{\alpha\beta} = C_{\alpha\beta\gamma\delta}\ \varepsilon_{\gamma\delta} \tag{50}$$

where $N_{\alpha\beta}$ are the components of the membrane surface stress, and $C_{\alpha\beta\gamma\delta}$ the constitutive tensor ($C = \frac{Eh}{1-\nu^2}$ is the tensile stiffness). The in-plane equilibrium equations are:

$$N_{\alpha\beta,\beta} + b_\alpha = \rho\ddot{u}_\alpha \tag{51}$$

and the out-of-plane equations are:

$$\left(N_{\alpha\beta}w_\beta\right)_{,\alpha} + b_3 + N_{\alpha\beta}\ z_{,\alpha\beta} = \rho\ddot{w} \tag{52}$$

The boundary conditions on the boundary where displacements are prescribed (Γ_u, Γ_w) are $u_\alpha = \overline{u}_\alpha$and $w = \overline{w}$, and the boundary conditions on the boundary where tractions are prescribed $(\Gamma_\sigma, \Gamma_v)$ are $N_{\alpha\beta}n_\beta = \overline{p}_\alpha$ and $\overline{V}_n = V_n$, respectively.

Using a weighted residual approach, we may write the in-plane and out-of-plane equilibrium as:

$$\begin{aligned} &\int_\Omega \left(N_{\alpha\beta,\beta} + b_\alpha - \rho\ddot{u}_\alpha\right) u_\alpha^* d\Omega = \\ &\int_{\Gamma_\sigma} \left(p_\alpha - \overline{p}_\alpha\right) u_\alpha^* d\Gamma + \\ &\int_{\Gamma_u} \left(\overline{u}_\alpha - u_\alpha\right) p_\alpha^* \left(u_\sigma^*\right) d\Gamma \end{aligned} \tag{53}$$

and

$$\begin{aligned} &\int_\Omega \left[\left(N_{\alpha\beta}w_\beta\right)_{,\alpha} - \frac{N_{\alpha\beta}}{R_{\alpha\beta}} + \left(b_3 - \rho\ddot{w}\right)\right] w^* d\Omega \\ &= \int_{\Gamma_V} \left(\overline{V}_n - V_n\right) w^* d\Gamma + \int_{\Gamma_w} \left(w - \overline{w}\right) V_n^* d\Gamma \end{aligned} \tag{54}$$

where $(\cdot)^*$ denote test function in stress and displacements.

Using the compatibility equations on the constitutive equations (i.e., compatibility is satisfied a priori), the surface stresses may be written as the sum of a linear part and a nonlinear part as follows:

$$N_{\alpha\beta} = N'_{\alpha\beta} + N^{(n)}_{\alpha\beta} + C\kappa_{\alpha\beta}w \tag{55}$$

where $N'_{\alpha\beta}$ is the linear part

$$\begin{aligned} N'_{11} &= C\left(u_{1,1} + \nu u_{2,2}\right) \\ N'_{22} &= C\left(u_{2,2} + \nu u_{1,1}\right) \\ N'_{12} &= \frac{1}{2}C\left(1-\nu\right)\left(u_{1,2} + u_{2,1}\right) \end{aligned} \tag{56}$$

$N^{(n)}_{\alpha\beta}$ is the nonlinear part

$$\begin{aligned} N^{(n)}_{11} &= \frac{C}{2}\left(w_{,1}^2 + \nu w_{,2}^2\right) \\ N^{(n)}_{22} &= \frac{C}{2}\left(w_{,2}^2 + \nu w_{,1}^2\right) \\ N^{(n)}_{11} &= \frac{1}{2}C\left(1-\nu\right) w_{,1}w_{,2} \end{aligned} \tag{57}$$

and

$$\begin{aligned} \kappa_{11} &= \frac{1}{R_{11}} + \nu\frac{1}{R_{22}} \\ \kappa_{22} &= \frac{1}{R_{22}} + \nu\frac{1}{R_{11}} \\ \kappa_{12} &= \frac{1-\nu}{R_{12}} \end{aligned} \tag{58}$$

Since the material is linear elastic and isotropic, we may write that

$$N'_{\alpha\beta}u^*_{\alpha,\beta} = C_{\alpha\beta\gamma\delta}\ u_{\gamma,\delta}u^*_{\alpha,\beta} = N'^*_{\gamma\delta}\left(u^*_\eta\right) u_{\gamma,\delta} \tag{59}$$

where $N'^*_{\gamma\delta} = C_{\alpha\beta\gamma\delta}\ u^*_{\alpha,\beta}$. Also, since $N_{\alpha\beta}n_\beta = p_\alpha$, we may write that

$$p_\alpha = N'_{\alpha\beta}n_\beta + N^{(n)}_{\alpha\beta}n_\beta + C\kappa_{\alpha\beta}wn_\beta \tag{60}$$

Also define $\hat{p}_\alpha = (p_\alpha, \overline{p}_\alpha)$, $\hat{u}_\alpha = (u_\alpha, \overline{u}_\alpha)$ on $(\Gamma_u, \Gamma_\sigma)$, and $N^*_{\alpha\beta}n_\beta = p^*_\alpha$

Using the divergence (Gauss) theorem on eq.53 and on eq. 54, and after some tedious algebra, one obtains the modified variational statements

$$\begin{aligned} 0 = &\int_\Omega \left[N'^*_{\alpha\beta}\left(u^*_\sigma\right)_{,\beta}u_\alpha\right] d\Omega + \\ &\int_\Omega \left(b_\alpha - \rho\ddot{u}_\alpha\right) u^*_\alpha d\Omega - \\ &\int_\Omega \left[N^{(n)}_{\alpha\beta}u^*_{a,\beta}\right] d\Omega - \\ &\int_{\Gamma_\sigma} \hat{p}_\alpha u^*_\alpha d\Gamma + \int_{\Gamma_u} \hat{u}_\alpha p^*_\alpha d\Gamma \end{aligned} \tag{61}$$

and

$$0 = \int_\Omega \left[-\frac{N^{(n)}_{\alpha\beta}}{R_{\alpha\beta}} + (b_3 - \rho\ddot{w}) \right] w^* d\Omega - \int_\Omega \left[(N_{\alpha\beta} w_{,\beta}) w^*_{,\alpha} \right] d\Omega + \int_\Omega \left[N_{\alpha\beta} w_{,\beta} n_\alpha w^* \right] d\Omega - \int_{\Gamma_V} \left(\overline{V}_n - V_n \right) w^* d\Gamma - \int_{\Gamma_w} (w - \overline{w}) V^*_n d\Gamma \quad (62)$$

In this form, these equations maybe written in incremental form, so that the residual vector and the tangent stiffness can be derived. In this mixed formulation, the stresses $\left(N'^*_{\alpha\beta}, N^{(n)}_{\alpha\beta}, p^*_\alpha, V^*_n\right)$ may be interpolated with interpolation functions of lower order than the displacements, making the formulation easier to implement. In-plane and bending-type stresses are included automatically. Follower type loads can also be included in the b_α vector.

V. Solution algorithms for static and dynamic analysis

In order to compute the initial shape of the membrane after inflation, the following static nonlinear analysis procedure is followed:

- apply the pressure load, and compute the residual vector **res** and tangent stiffness matrix $\mathbf{K_T}$;
- solve for the displacement increment as $\Delta\mathbf{q} = \mathbf{K_T^{-1}} \cdot \mathbf{res}$;
- update displacements to $\mathbf{q_{new}} = \mathbf{q_{old}} + \Delta\mathbf{q}$;
- check norm of **res** or norm of $\Delta\mathbf{q}$ as a check of convergence;
- if norms are within tolerance, apply next load step, otherwise continue the iteration.

The dynamic equilibrium analysis, also required for control analysis, is slightly different, and proceeds as follows:

- given the equilibrium solution (state vector) in terms of nodal displacements $\mathbf{q}$ and velocities $\dot{\mathbf{q}}$, use the global stiffness matrix $\mathbf{K_T}$ computed at time t to compute the nodal loads from $\mathbf{f} = \mathbf{K_T} \cdot \mathbf{q}$;
- compute the global mass matrix, the global stiffness matrix (including initial stress terms), the global damping matrix, and the external force vector, including control force terms at time $t + dt$;
- update the state vector according to the time integration scheme (a possible chice is a Newmark type predictor-corrector scheme);
- check that the residual of forces (internal less external forces) at time $t + dt$ is smaller than a pre-set tolerance, otherwise recompute;
- go to the next time step.

All these methods can be considered to be homotopy methods. More generally, a solution method capable of tracing geometric or material instabilities such as singularities of the tangent stiffness matrix must be homotopic in nature.

VI. Some applications

A. ARISE Spacecraft model

In this case half of an inflatable envelope is metallized to reflect both RF and sunlight. A simple model of the ARISE inflatable antenna was built in IMOS. The simulation model of the ARISE spacecraft is shown in Figure 6. The lenticular envelope is supported by a torus, which is joined to a spacecraft bus by struts (3 here). The torus and struts are to be inflatable, but later rigidized (e.g. by cooling past the glass transition temperature). The model is an off axis parabolic reflector, with scalable diameter, and focal length $f = D/2$. The finite element mesh model, shown in Figure 6, uses Bernoulli-Euler beam elements to model the struts and torus. A simple circular mesh generator was added to IMOS to allow a set of plate or membrane elements to model the lenticular structure. Once the model was built, mode shapes were generated. Representative material properties were used for this $25m$ diameter case. Figure 7 shows the input excitation given by a specified command of one of the reaction wheels located on the spacecraft bus. Figure 8 shows the dynamic deformation at one point on the torus, also modeled with beam finite elements. A more detailed simulation using the membrane elements developed in Part 1 of this paper will be described in Part 2.

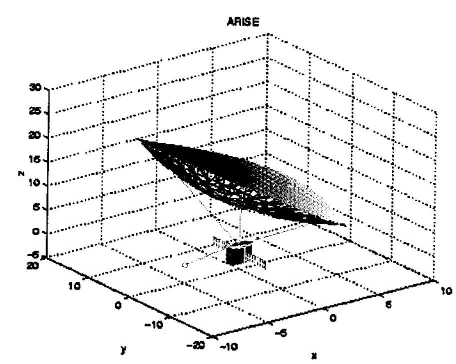

Figure 6. ARISE simulation model.

B. Inflatable modeling package for IMOS

Various options were considered here for the membrane modeling, and were developed for IMOS to at least a theoretical level. Early efforts included a linear shell element; a linear membrane element with tension; a shell element with pre-stress. These isoparametric [2] elements are capable of providing accurate results in the small deformation regime, but may be used within a corotational formulation for large deformations. After these investigations we decided upon developing a nonlinear membrane shell element based upon previous work in the area of rubberlike models. The element uses nonlinear kinematics and a linear material constitutive equation and so is capable of modeling large deformations. Both 3 and 6 node triangular versions of the element have been coded into matlab/IMOS. Using the principle of virtual work, the residual and tangent stiffness are derived including effects of pre-stress, geometric nonlinearities, pressure, and follower loads. These development have been extensively described in the previous sections of this paper. Using a homotopy approach, we have simulated the inflation process (Figure 9), and effects of boundary changes including control forces. Code has been developed to determine surface displacements upon application of the inflation pressure. Figure 10 shows the displacement of the torus when the surface is constrained to be on a parabolois. The code also computes surface errors in an rms sense, and decomposes the surface error into Zernike polynomials, as shown in Figure 11. More details on these numerical developments will be described in Part 2 of this paper.

VII. Control and Stabilization Options for Gossamer Spacecraft

Given the above element some limited shape control experiments have been done to investigate the effectiveness of turnbuckles for control. While turnbuckles cannot remove all surface errors (in particular the errors in inflating a uniform, flat membrane) they are quite effective in reducing errors such as those created by incorrect deployment of the torus structure. More details on shape control of membrane reflectors will be will be discussed in Part 2 of this paper.

Robust and realistic control, sensing, estimation, and system identification methodologies and algorithms are common to most of the gossamer spacecraft envisioned in NASA missions. This commonality stems from the fact that their control design and performance is very sensitive to modeling errors. These may arise from unmodeled flexibility in large structures, unmodeled sensor and actuator dynamics, and uncertainties in the interaction with the environment. The long life expectancy of these envisioned missions (3 to 5 years) requires a sensing and actuation scheme which must be robust to uncertainties in the plant model. There is a variety of dynamics and control issues associated with gossamer-like spacecraft, which have only begun to be addressed. Some are common to other spacecraft as well, but in general they present additional problems. In general, the control problem for gossamer spacecraft is multifaceted [4], [5], [6], [7], [8], [9], [10]. There exist problems arising from shape errors originating in manufacturing errors, fabrication errors, and errors deriving from dynamic noise and ageing. In terms of attitude control, as structures get larger, and more flexible, control-structure interaction becomes the dominant cause for possible instability. Translational control becomes necessary if the gossamer spacecraft must fly in a formation. Pointing control is very demanding when inflatable apertures are used in interferometric instruments. Momentum control becomes necessary to compensate for solar pressure disturbances. Shape control represents a challenge for maintenance of surface accuracy. Deployment control is advisable, since inflatable structures are tightly packaged with tendency to crease formation in the film material, which has an influence on the deployment trajectory. Specifically:

- Attitude Stabilization and Pointing Control: solar sail, sunshades, and inflatable reflector structures are light, possibly very large, and hence simultaneously quite flexible. The pointing issues of large flexible spacecraft cannot be addressed as if they were more traditional structures. The problem is difficult because a high control bandwidth is necessary for tight requirements, relative to the low frequency structural modes.
- Momentum Control: One issue is that solar torques will be large because the surface is large and opaque, and the center of pressure to center of mass offset is also large. This can lead to substantial propellant requirements to maintain pointing, as in the ARISE study. For very large reflectors, the propellant mass alone could be prohibitive.
- Shape Control: To control the shape of a sunshield, solar power array, or an inflatable reflector there are a variety of techniques that have been considered, but none have been demonstrated in flight: active turnbuckles, cable networks, piezo-electric polymer membrane - PVDF, piezo-optical polymer membrane, electrochromic patches, and laser keratectomy. In general, the membrane must be supported by a frame, possibly an inflatable ring or torus. The membrane itself may have a rim or serpentine structure that distributes the attachment load over the thin membrane. Recently, constant-force springs have been proposed for use to make the membrane less sensitive to the deployed position of the torus.
- Thrust Vector/Steering Control: this type of control is very specific to solar sails, and results from a combination of both deltaV control and attitude control required to keep the sail pointed towards the Sun.

VIII. Conclusions

The purpose of this paper is to shed some light on the dynamics and control problems one faces when modeling and analyzing gossamer-type spacecraft such as antennas built from inflatable structures, reflecting surfaces such as solar sails, and heat control surfaces such as solar shields. Using finite elements, I have derived the incremental equations of motion for a membrane to be used in simulations of precision inflatable structures. A boundary integral formulation has also been presented, as a promising alternative to the finite element derivation. Some numerical results obtained with the formulation outlined in this paper are also presented. A discussion on control problems posed by large membrane structures in space will be included in Part 2.

Achnowledgement The research described in this paper was carrieed out at the Jet Propulsion Laboratory, California Institute of Technology, under a contract with the National Aeronautics and Space Administration.

References

[1] Campbell, J.D.: *On the Theory of Initially Tensioned Circular Membranes Subjected to Uniform Pressure*, Quarterly Journal of Mechanics and Applied Mathematics, vol. IX, part 1, 1956, pages 84-93.

[2] Cook, R. D.: *Concepts and Applications of Finite Element Analysis*, John Wiley & Sons, 1989.

[3] Gruttmann, F. and Taylor, R. L.: *Theory and Finite Element Formulation of Rubberlike Membrane Shells using Prin-*

cipal Stretches, International Journal for Numerical Methods in Engineering, vol.35, pages 1111-1126, 1992.

[4] Murphy, L.M.: *Moderate Axisymmetric Deformations of Optical Membrane Surfaces*, Journal of Solar Energy Engineering, May 1987, vol. 109, pages 111-120.

[5] Okubo, H., Komatsu N., and Tsumura T.: *Tendon Control System for Active Shape Control of Flexible Space Structures*, Jounal of Intelligent Material Systems and Structures, Vol. 7, July 1996.

[6] Shahin A.R., Meckl P.H., and Jones J.D.: *Modeling of SMA Tendons for Active Control of Structures*, Jounal of Intelligent Material Systems and Structures, Vol. 8, January 1997.

[7] Shimizu M.: *Study of Shape Control for Modular Mesh Antenna*, Electronics and Communications in Japan, Part 1, Vol. 79, No. 12, 1996.

[8] Tabata T., and Natori M.C.: *Active Shape Control of a Deployable Space Antenna Reflector*, Journal of Intelligent Material Systems and Structures, Vol. 7, March 1996.

[9] Vaughan, H.: *Pressurising a Prestretched Membrane to form a Paraboloid*, International Journal of Engineering Sciences, vol 18, 1980, pp99-107.

[10] You, Z.: *Displacement control of prestressed structures*, Computer Methods in Applied Mechanics and Engineering, vol.144, 1997, pp 51-57.

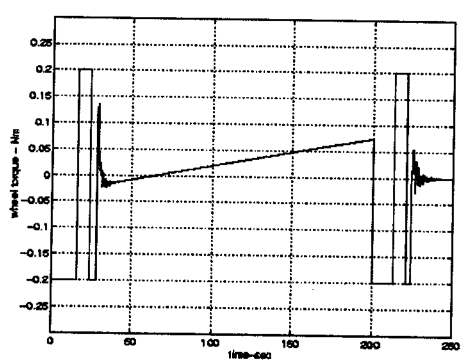

Figure 7. Excitation Input: reaction wheel torque for re-orientation vs. time.

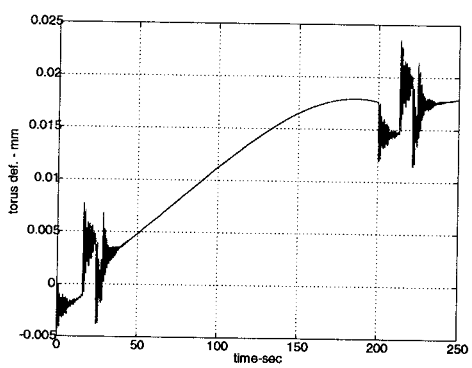

Figure 8. Deformation of torus edge vs. time.

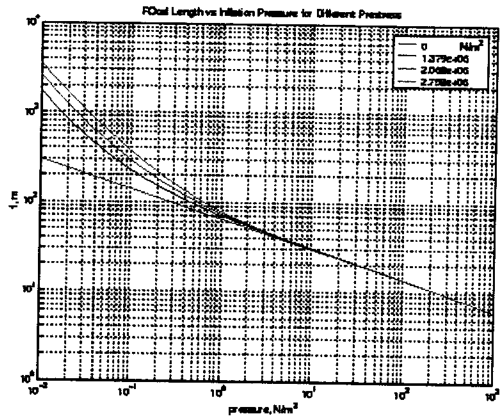

Figure 9. Focal Length vs. Inflation Pressure for Different Pre-stress levels.

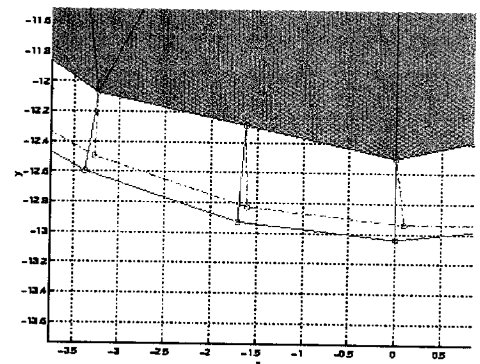

Figure 10. Displacement of torus and constant force springs under inflation pressure in order for the reflector to produce a parabolic surface.

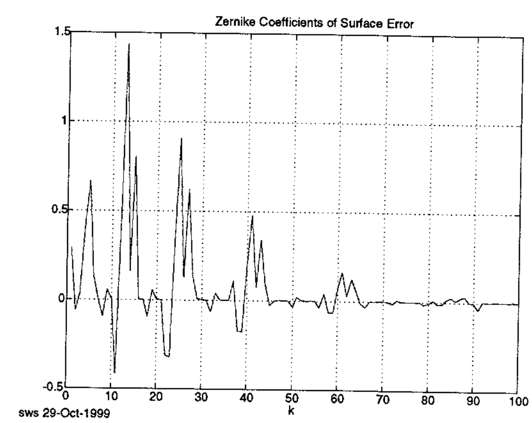

Figure 11. Zernike's coefficients of surface error of inflatable lenticular dish.